



CrossMark
click for updates

Cite this: *RSC Adv.*, 2016, 6, 111399

Controlling the selectivity of catalytic oxidation of styrene over nanocluster catalysts†

Jinsong Chai,^a Hanbao Chong,^c Shuxin Wang,^b Sha Yang,^b Mingzai Wu^{*a} and Manzhou Zhu^{*b}

Atomically precise Au₂₅ and Ag₄₄ as well as alloy nanoclusters (Au_{25-x}Ag_x and Au₁₂Ag₃₂) are investigated for catalytically selective oxidation of styrene. Distinct synergistic effects of Au–Ag bimetallic nanoclusters are identified. In addition, the addition of H₂O (a few vol%) to the reaction solvent is found to drastically affect the product selectivity. Based upon Fourier transform infrared (FT-IR) and X-ray photoelectron spectroscopy (XPS) measurements, a possible mechanism for the nanocluster-catalyzed styrene selective oxidation is proposed. Specifically, H₂O could change the surface composition of Au on the Au₂₅ nanocluster and the valence state of Ag on the Ag₄₄ nanocluster. Such effects are also present on the bimetallic Au_{25-x}Ag_x, but not on the bimetallic Au₁₂Ag₃₂ nanocluster because for the latter Au exclusively acts as kernel atoms. This work provides insights into the different functional roles of water in the nanoclusters based upon their different atomic structures.

Received 15th September 2016
Accepted 11th November 2016

DOI: 10.1039/c6ra23014h

www.rsc.org/advances

1 Introduction

Alloys often exhibit unique properties compared to the single component systems.^{1–6} Interactions between different atoms can modify the alloy's electronic structure and surface composition, and lead to enhanced chemical and physical properties.^{7–11} Recently, fascinating optical,^{12–14} electronic,^{15,16} and catalytic^{17–19} properties have been reported for bimetallic nanostructures composed of noble metals such as gold (Au), silver (Ag), platinum (Pt), and palladium (Pd). Such alloy nanostructures offer a wide range of applications, including surface-enhanced Raman scattering (SERS),^{20,21} biosensors,^{22,23} catalysis^{17,18} and many others.^{24,25} In recent years, atomically precise metal nanoclusters have emerged as a new type of nanomaterials and attracted significant research interest due to their well-determined structures which benefit the deep mechanistic understanding. According to the recent studies, substitution with heteroatoms can drastically affect the catalytic properties of alloy nanoclusters. For example, Pt₁Au₂₄(SC₂H₄-Ph)₁₈ with single Pt atom doped into gold nanoclusters (NCs), was reported by Jin and co-workers, and it exhibits largely improved catalytic performance than Au₂₅(SR)₁₈ for styrene

oxidation.¹⁷ Tsukuda and co-workers found that single Pd doping significantly boosts the performance of Au₂₅ in aerobic alcohol oxidation.¹⁸

So far, Ag–Au bimetallic nanostructures represent one of the most extensively investigated categories because they can possibly reduce the cost of the Au catalysts and enhance the catalytic performance.^{26–30} Various gold and silver nanoparticles have been made and used as catalysts in recent years. For example, Au–Ag bimetallic particles exhibit better catalytic performance than their monometallic counterparts in producing H₂O₂ from an O₂-saturated ethanol/water mixture under UV irradiation.³¹ Recently, small mixed-metal clusters have been synthesized by doping Ag into atomically precise Au_n nanoclusters.^{32–36} Our group studied the catalytic activity of Ag–Au bimetallic nanoclusters (*e.g.* Au₂₄Ag₄₆(SR)₃₂ and Au₁₂Ag₃₂(SR)₃₀) with different structures on styrene oxidation.³⁷ Generally, Ag gives higher selectivity for benzaldehyde and Au favours better conversion, while in the case of Au₂₄Ag₄₆/CNT (where, CNT = carbon nanotubes) both advantages are amplified.³⁷

A well-known phenomenon in nanogold catalysis is that in the O₂-involved reactions (such as CO oxidation, alcohol oxidation, and propene epoxidation), water (typically in the form of vapour) was found to be significant in determining the conversion efficiency.^{38–47} Therefore, deep understanding on the water effect in catalysis is of great importance. To this end, we use styrene oxidation as a model reaction to explore the detailed interactions between water and nanoclusters.

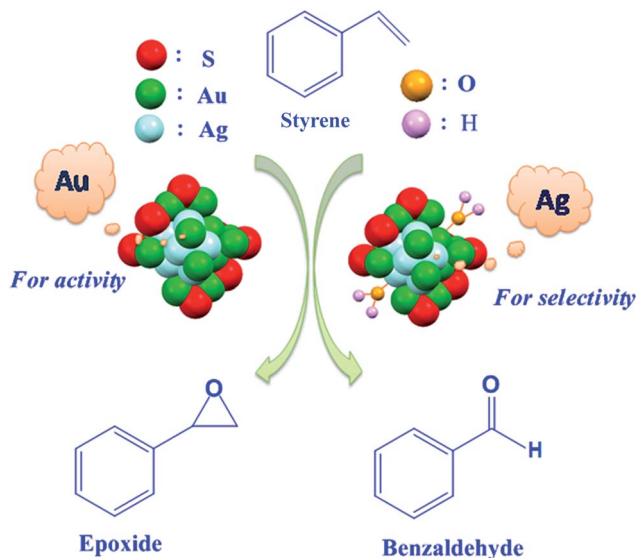
Herein, the catalytic performance of structure-determined homometal and alloyed nanoclusters were examined for the reaction of styrene selective oxidation. *tert*-Butyl hydroperoxide (TBHP) is used as the oxygen source and toluene as the

^aSchool of Physics and Materials Science, Anhui University, Hefei, Anhui, 230601, P. R. China. E-mail: mingzaiwu@gmail.com

^bDepartment of Chemistry and Centre for Atomic Engineering of Advanced Materials, Anhui University, Hefei, Anhui, 230601, P. R. China. E-mail: zmz@ahu.edu.cn

^cModern Experiment and Technology Center, Anhui University, Hefei, Anhui, 230601, P. R. China

† Electronic supplementary information (ESI) available: Detailed information about the synthesis, optical absorption spectrum of nanoclusters, synthesis and catalytic test of nanoparticles, Table S1, Fig. S1–S8. See DOI: 10.1039/c6ra23014h



Scheme 1 Catalytic selective oxidation of styrene over $\text{Au}_{25-x}\text{Ag}_x/\text{CNT}$ (color labels: green = Au, light blue = Ag, red = S, golden = O and magenta = H).

solvent. The mixed solvents of toluene and water are then used for comparison and probing the water effect. Interestingly, H_2O is found to dominate the change of selectivity (Scheme 1). The Fourier transform infrared (FT-IR) spectroscopic analysis and X-ray photoelectron spectroscopy (XPS) measurements are then carried out to investigate the major roles of water in the catalytic reaction. Atomic level mechanistic insight into the nanocluster-catalysed selective styrene oxidation is further obtained.

2 Experimental section

2.1 Chemicals

All chemicals were purchased from commercial sources and used without further treatments. All solvents were of chromatographic grade. Tetrachloroauric(III) acid ($\text{HAuCl}_4 \cdot 3\text{H}_2\text{O}$, >99.99% metals basis), AgNO_3 , and sodium borohydride (>98%) were purchased from ACROS Organic. Phenylethanethiol and 3,4-difluorothiophenol ($\geq 97\%$) were from Aldrich. Toluene (HPLC grade, $\geq 99.9\%$, Aldrich), ethanol (HPLC grade, $\geq 99.9\%$) and other solvents were from Aldrich. Pure water was ordered from Wahaha Co LTD and $^{18}\text{OH}_2$ (97% atom ^{18}O) were from Aldrich. Carbon nanotubes were from Beijing Bo Yu high-tech new material technology co., LTD.

2.2 Synthesis of $\text{Au}_{25}(\text{SR})_{18}$, $\text{Au}_{25-x}\text{Ag}_x(\text{SR})_{18}$, $\text{Ag}_{44}(\text{SR})_{30}$ and $\text{Au}_{12}\text{Ag}_{32}(\text{SR})_{30}$

We first prepared the 25-atom $\text{Au}_{25}(\text{SR})_{18}$ and $\text{Au}_{25-x}\text{Ag}_x(\text{SR})_{18}$ ($x = 1-9$) nanoclusters using our previously reported methods.^{32,48} The $\text{Ag}_{44}(\text{SR})_{30}$ and $\text{Au}_{12}\text{Ag}_{32}(\text{SR})_{30}$ nanoclusters were prepared using the procedures reported by Zheng *et al.*³⁶ The synthetic details are provided in the ESI.†

2.3 Catalyst preparation and characterization

Preparation of catalysts. $\text{Au}_{25}(\text{SR})_{18}$, $\text{Au}_{25-x}\text{Ag}_x(\text{SR})_{18}$, $\text{Ag}_{44}(\text{SR})_{30}$ and $\text{Au}_{12}\text{Ag}_{32}(\text{SR})_{30}$ were supported on commercial carbon nanotubes (Beijing Bo Yu high-tech new material technology co., LTD). The CNTs were first dispersed in toluene, and nanoclusters were added to the suspension of CNTs under vigorous magnetic stirring. The adsorption of nanoclusters was allowed to proceed overnight. Then the product was separated from the solution by centrifugation. The cluster/CNT composite was dried in vacuum for 12 h. Calcination of the $\text{Au}_{25}\text{SR}/\text{CNT}$, $\text{Au}_{25-x}\text{Ag}_x\text{SR}/\text{CNT}$, $\text{Ag}_{44}\text{SR}/\text{CNT}$, and $\text{Au}_{12}\text{Ag}_{32}\text{SR}/\text{CNT}$ was performed in a quartz-tube oven under vacuum at 200°C .

Catalytic test. A 10 mL Schlenk bottle was charged with 0.5 mmol styrene and 1.5 mmol TBHP, 20 mg cluster/CNT catalyst and 10 mg K_2CO_3 , 2 mL solvent. Then the suspension was stirred at 65°C for reaction. After the reaction, the suspension was centrifuged to remove solid, and catalytic product was analysed by gas chromatography with internal standard.

Characterization. The UV-vis absorption spectra were recorded on UV-vis spectrophotometer (Agilent). The catalysts were investigated by transmission electron microscopy (TEM) on a JEM 2100 microscope. Time-conversion data were collected by a GC 2010 plus (from Shimadzu) and a GC-MS saturn 2200 (from Varian). To analyse whether the catalysts interacted with water or not, we soaked the catalysts in water for 24 hours and then dried the catalysts in an oven to remove the water adhered to the surface of catalysts. The catalysts were analyzed Fourier transform infrared (FT-IR) spectroscopy on a Bruker VERTEX80+HYPERION000. The X-ray photoelectron spectroscopy (XPS) measurements were performed on an ESCALAB 250 high-performance electron spectrometer with monochromated Al $\text{K}\alpha$ radiation as the excitation source.

3 Results and discussion

3.1 Characterization of the catalysts

The nanoclusters including $\text{Au}_{25}(\text{SR})_{18}$,⁴⁸ $\text{Au}_{25-x}\text{Ag}_x(\text{SR})_{18}$ ($x = 1-9$),³² $\text{Ag}_{44}(\text{SR})_{30}$,³⁶ and $\text{Au}_{12}\text{Ag}_{32}(\text{SR})_{30}$ (ref. 36) were first prepared using the previously reported methods. Fig. 1a and c show the crystal structures of homogold $\text{Au}_{25}(\text{SR})_{18}$ nanoclusters and homosilver $\text{Ag}_{44}(\text{SR})_{30}$ nanoclusters, respectively. The crystal structure of surface-doped Ag–Au bimetallic nanoclusters $\text{Au}_{25-x}\text{Ag}_x(\text{SR})_{18}$ is shown in Fig. 1b and d shows the crystal structure of the core–shell structured $\text{Au}_{12}\text{Ag}_{32}(\text{SR})_{30}$ nanocluster with an Au_{12} kernel and an Ag_{32} shell. The purity of these nanoclusters was verified by comparing their UV-vis absorption spectra with standard ones reported^{32,36,48} (Fig. S1†).

Carbon nanotubes (CNT) were used as the support for the nanoclusters since carbon does not strongly interact with gold while transition metal oxide supports often exhibit strong interactions with gold nanoparticles. In addition, CNTs have an advantage of preventing diffusion of naked nanoclusters.⁴⁹ After wet deposition of nanoclusters onto CNT, $\text{Au}_{25}\text{SR}/\text{CNT}$, $\text{Au}_{25-x}\text{Ag}_x\text{SR}/\text{CNT}$, $\text{Ag}_{44}\text{SR}/\text{CNT}$ and $\text{Au}_{12}\text{Ag}_{32}\text{SR}/\text{CNT}$ composites were collected by centrifugation. The supernatant was colourless, indicating that the clusters were completely

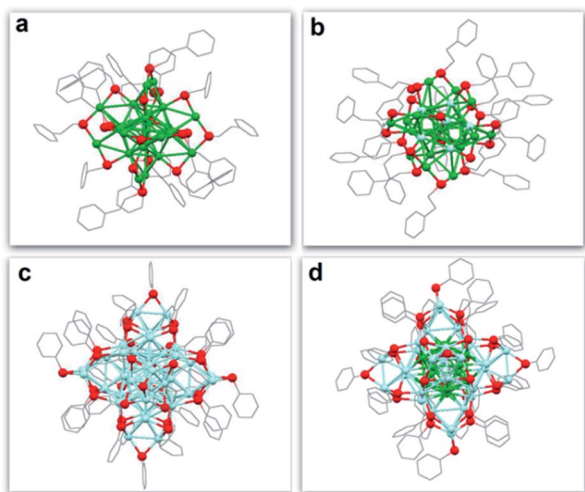


Fig. 1 Crystal structures of (a) $\text{Au}_{25}(\text{SR})_{18}$; (b) $\text{Au}_{25-x}\text{Ag}_x(\text{SR})_{18}$; (c) $\text{Ag}_{44}(\text{SR})_{30}$; (d) $\text{Au}_{12}\text{Ag}_{32}(\text{SR})_{30}$ (color labels: green = Au, light blue = Ag, red = S, gray stick = C; all H atoms are not shown).

adsorbed onto the CNTs. The hydrophobicity of clusters and CNTs led to the efficient absorption of nanoclusters on CNTs. The solids were dried in vacuum for 12 h. TEM images of $\text{Au}_{25}(\text{SR})_{18}$, $\text{Au}_{25-x}\text{Ag}_x(\text{SR})_{18}$, $\text{Ag}_{44}(\text{SR})_{30}$ and $\text{Au}_{12}\text{Ag}_{32}(\text{SR})_{30}$ (Fig. 2) showed that the clusters were adsorbed on the surface of CNTs, and the size range is 0.8–1.6 nm.

3.2 Selective oxidation of styrene

The $\text{Au}_{25}/\text{CNT}$, $\text{Au}_{25-x}\text{Ag}_x/\text{CNT}$, $\text{Ag}_{44}/\text{CNT}$ and $\text{Au}_{12}\text{Ag}_{32}/\text{CNT}$ catalysts were investigated for the selective oxidation of styrene (Table 1). TBHP was used as the oxygen source and toluene as the solvent. The results imply that epoxide is the predominant product and benzaldehyde as the main side-product, while other products are minor (Table 1, entries 1–4).^{50–52} Among the catalysts, homogold $\text{Au}_{25}/\text{CNT}$ showed a higher conversion of styrene (78.9%) than the homosilver $\text{Ag}_{44}/\text{CNT}$ 49.9%. The

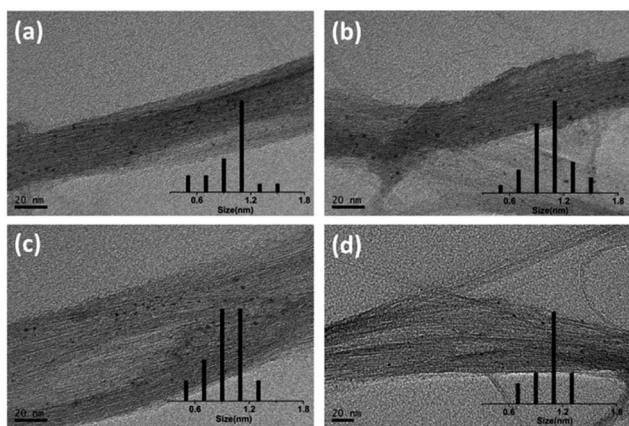


Fig. 2 Typical TEM images and cluster size distributions of (a) $\text{Au}_{25}:\text{SR}/\text{CNT}$, (b) $\text{Au}_{25-x}\text{Ag}_x:\text{SR}/\text{CNT}$, (c) $\text{Ag}_{44}:\text{SR}/\text{CNT}$, (d) $\text{Au}_{12}\text{Ag}_{32}:\text{SR}/\text{CNT}$. CNT = carbon nanotubes.

selectivity for epoxide is 63.9% over $\text{Au}_{25}/\text{CNT}$ and the homogold $\text{Ag}_{44}/\text{CNT}$ showed the highest selectivity for epoxide (74.5%), despite its lower conversion of styrene (49.9%).

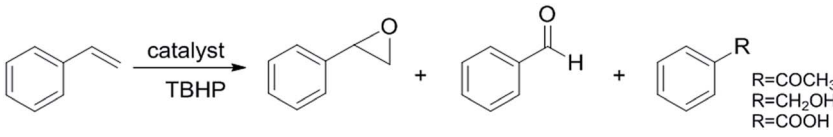
In this reaction, the bimetallic nanoclusters clearly show synergistic effects in activity and/or selectivity. For the 25-atom catalysts (Table 1, entries 1 and 3), the selectivity for epoxide was increased from 63.9% over homogold $\text{Au}_{25}/\text{CNT}$ to 74.3% over $\text{Au}_{25-x}\text{Ag}_x/\text{CNT}$ with a comparable activity. In contrast, for the 44-atom catalysts, the bimetallic $\text{Au}_{12}\text{Ag}_{32}/\text{CNT}$ nanocluster largely improves the conversion of styrene relative to $\text{Ag}_{44}/\text{CNT}$ (74.5% vs. 49.9%) but the epoxide selectivity is less (60.0% vs. 74.5%).

An intriguing effect of water was discovered in our catalytic reaction system when using a mixed solution of water and toluene as the solvent (Table 1, entries 5–8). Similar to the observations in entries 1–4 (without water), the homogold $\text{Au}_{25}/\text{CNT}$ had a higher conversion of styrene (78.3%) than the $\text{Ag}_{44}/\text{CNT}$ catalyst (45.1%), see Table 1 entries 5 and 6. After adding water to the solvent, the selectivity for product was drastically changed; benzaldehyde (instead of epoxide) becomes the predominant product. Especially for $\text{Ag}_{44}/\text{CNT}$ and $\text{Au}_{25-x}\text{Ag}_x/\text{CNT}$ (entries 6 and 7), the selectivity is as high as 94.5% and 95.9%, respectively. Interestingly, the $\text{Au}_{12}\text{Ag}_{32}/\text{CNT}$ catalyst still retains the selectivity for epoxide (entry 8) which is comparable to that of the case of no water. In addition, we also have synthesized a series of nanoparticles of size 2–8 nm (Fig. S8†) and used them as catalysts for selective oxidation of styrene. The results (Table S1†) show no effect of water on the selectivity of styrene oxidation, nor the conversion of styrene. Therefore, the nanoclusters are unique in exhibiting the water effect on controlling the selectivity of styrene oxidation.

To verify the aforementioned proposal, mixed solvents containing different proportions of water and toluene were used. We added 0, 20, 40, 60, and 100 μL H_2O into 1.5 mL toluene, respectively. As shown in Fig. 3, the selectivity to benzaldehyde increases with the addition of water into the solvent (Fig. 3a), while the selectivity toward epoxide decreases accordingly (Fig. 3b). However, the catalytic performance of the bimetallic core-shell structured $\text{Au}_{12}\text{Ag}_{32}/\text{CNT}$ nanocluster catalyst is distinctly different from the $\text{Au}_{25-x}\text{Ag}_x/\text{CNT}$ catalyst, as $\text{Au}_{12}\text{Ag}_{32}$ maintains a nearly constant selectivity for epoxide in different mixed solvents (Fig. 3, blue line).

3.3 Mechanism of styrene oxidation on catalysts

Taking together the above experimental results, we rationalize that water induces the change of the catalytic selectivity *via* two possible pathways: (1) water reacts with epoxide to form benzaldehyde; (2) water reacts with catalysts and leads to some change of catalysts. To test the first pathway, we performed the hydrolysis reaction of epoxide using CNT (control), $\text{Au}_{25}/\text{CNT}$, $\text{Au}_{25-x}\text{Ag}_x/\text{CNT}$, $\text{Ag}_{44}/\text{CNT}$ and $\text{Au}_{12}\text{Ag}_{32}/\text{CNT}$ as catalysts, respectively (Table 2). Only trace amounts of benzaldehyde (the yields of benzaldehyde were <1%) were detected from the hydrolysis reaction of epoxide, thus, the hydrolysis pathway is irrelevant in our catalytic reaction, and instead the second pathway should be the dominant pathway. The results of selective oxidation reaction of styrene imply that the catalytic

Table 1 The catalytic performance of Au₂₅/CNT, Au_{25-x}Ag_x/CNT, Ag₄₄/CNT and Au₁₂Ag₃₂/CNT for the selective oxidation of styrene^a


Entry	Catalytic	Solvent	Conversion ^b (%)	Selectivity ^c (%)		
				Epoxide	Benzaldehyde	Other products
1	Au ₂₅ /CNT	Toluene	78.9	63.9	29.6	6.5
2	Ag ₄₄ /CNT	Toluene	49.9	74.5	17.4	8.1
3	Au _{25-x} Ag _x /CNT	Toluene	77.4	74.3	23.7	<3
4	Au ₁₂ Ag ₃₂ /CNT	Toluene	74.5	60.0	35.2	4.8
5	Au ₂₅ /CNT	Toluene and H ₂ O	78.3	19.3	73.9	6.8
6	Ag ₄₄ /CNT	Toluene and H ₂ O	45.1	5.1	94.5	<3
7	Au _{25-x} Ag _x /CNT	Toluene and H ₂ O	76.5	3.1	95.9	<3
8	Au ₁₂ Ag ₃₂ /CNT	Toluene and H ₂ O	74.4	56.8	41.2	<3

^a Reaction conditions: 20 mg catalyst, 2 wt% clusters loading, 57 μ L (0.5 mmol) styrene, 144 μ L (1.5 mmol) TBHP, 10 mg K₂CO₃, 2 mL solvent, 65 $^{\circ}$ C, 24 hours. ^b Conversion = (converted styrene)/(initial amount of styrene) \times 100. ^c Determined by gas chromatography with internal standard.

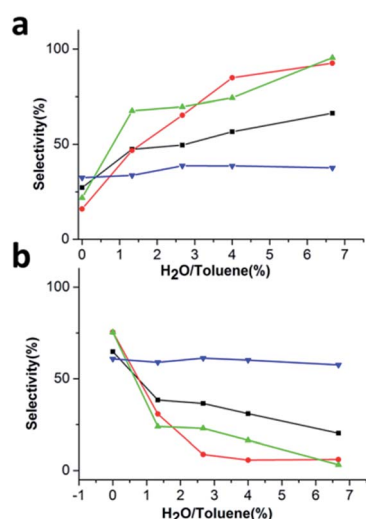


Fig. 3 (a) The benzaldehyde selectivity as a function of the volume percent of water. (b) The epoxide selectivity as a function of the vol% of water (color labels: black line = Au₂₅, red line = Au_{25-x}Ag_x, cyan line = Ag₄₄, blue line = Au₁₂Ag₃₂).

performance of the nanocluster catalysts correlate with their atomic structures (*i.e.* the locations of Au and Ag atoms). The interactions between the nanocluster and H₂O might be distinctly different for the different atomic structures. The Fourier transform infrared (FT-IR) spectroscopic analysis identified a band centred at 1630 cm⁻¹ (Fig. 4), which is assigned to the δ OH of co-adsorbed water.⁵³ Note that the peak at 1630 cm⁻¹ exists in all of these catalysts, indicating that water interacts with the surfaces of all of them.

X-ray photoelectron spectroscopy (XPS) measurements were then conducted to figure out the role of water. Fig. 5 displays the XPS spectra of Au₂₅/CNT, Ag₄₄/CNT, and Au_{25-x}Ag_x/CNT

Table 2 The hydrolysis reaction of epoxide^a


Entry	Catalytic	Solvent	Yield ^b (%)
1	CNT	Toluene and H ₂ O	<1
2	Ag ₄₄ /CNT	Toluene and H ₂ O	<1
3	Au _{25-x} Ag _x /CNT	Toluene and H ₂ O	<1
4	Au ₁₂ Ag ₃₂ /CNT	Toluene and H ₂ O	<1
5	Au ₂₅ /CNT	Toluene and H ₂ O	<1

^a Reaction conditions: 20 mg catalyst, 2 wt% clusters loading, 57 μ L (0.5 mmol) epoxide, 144 μ L (1.5 mmol) TBHP, 1.5 mL toluene and 100 μ L H₂O, 10 mg K₂CO₃, 65 $^{\circ}$ C, 24 h. ^b Determined by gas chromatography.

catalysts along with water-processed samples. The black line of Fig. 5a gives the XPS signal of Au₂₅/CNT without water, and the Au 4f_{7/2} binding energy is 83.98 eV. The binding energy of Au₂₅/CNT soaked by water (Fig. 5a, red line) is almost identical to that of Au₂₅/CNT without water. Therefore, the water adsorption on the surface of Au₂₅/CNT makes little influence on the valence state of Au. Similarly, the water does not change the valence state of Au in Au_{25-x}Ag_x/CNT catalyst, either (Fig. 5c). By contrast, the major influence of water on the valence state of Ag in both Ag₄₄ and Au_{25-x}Ag_x can be clearly seen from Fig. 5b and d. In Fig. 5b, the binding energy of Ag 3d_{5/2} in Ag₄₄/CNT increases from 367.78 eV (without water, black line) to 368.08 eV (with water, red line). In Fig. 5d, the shift of the Ag 3d_{5/2} peak in Au_{25-x}Ag_x/CNT changes from 367.88 eV to 368.48 eV. These data indicate the electron transfer from H₂O to Ag. Of note, the relationship between the binding energy positive shift and reduction of Ag is opposite to other elements.⁵⁴

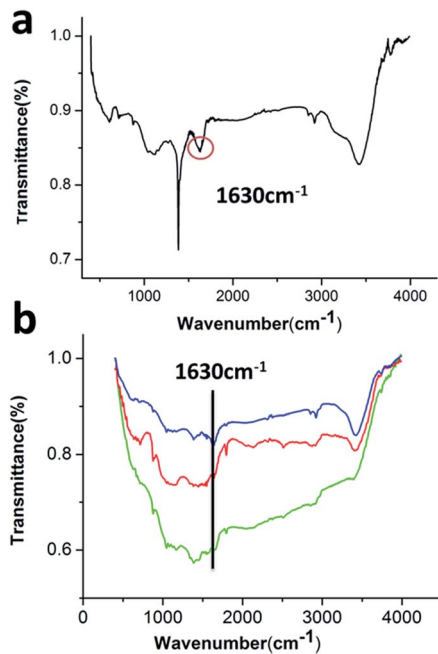


Fig. 4 (a) FT-IR spectrum of the $Au_{25-x}Ag_x/CNT$ which had been soaked with water. (b) FT-IR spectrum of soaked catalysts with water: black line, Ag_{44}/CNT ; red line, Au_{25}/CNT ; green line, $Au_{32}Ag_{12}/CNT$. The peak at 1630 cm^{-1} belongs to δOH of co-adsorbed water.

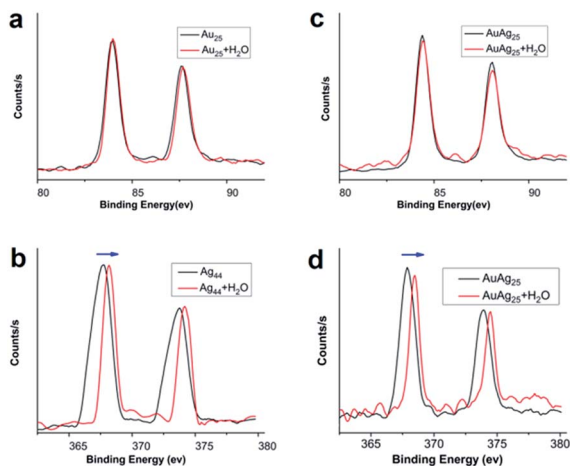


Fig. 5 The XPS spectra of (a) Au 4f for Au_{25}/CNT ; (b) Ag 3d for Ag_{44}/CNT ; (c) Au 4f for $Au_{25-x}Ag_x/CNT$; (d) Ag 3d for $Au_{25-x}Ag_x/CNT$.

In addition to the aforementioned analysis, the XPS measurements were also performed on $Au_{12}Ag_{32}/CNT$ samples and water-soaked $Au_{12}Ag_{32}/CNT$ samples. Similar to the observations in Fig. 5a and c, the water adsorption does not influence the binding energy of Au $4f_{7/2}$. To our surprise, H_2O does not make an obvious impact on the valence state of Ag in $Au_{12}Ag_{32}/CNT$, either (Fig. 6b).

From the XPS analysis, we proposed a possible mechanism for Au_{25} catalysed styrene oxidation (Scheme 2). The reaction starts with the binding of the oxidant TBHP onto the dry Au_{25}

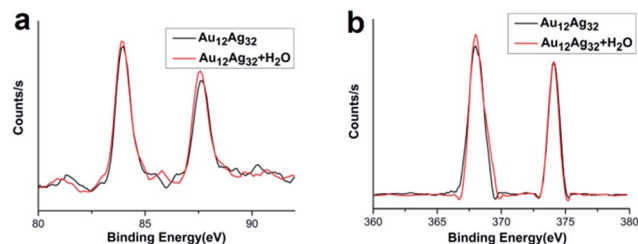
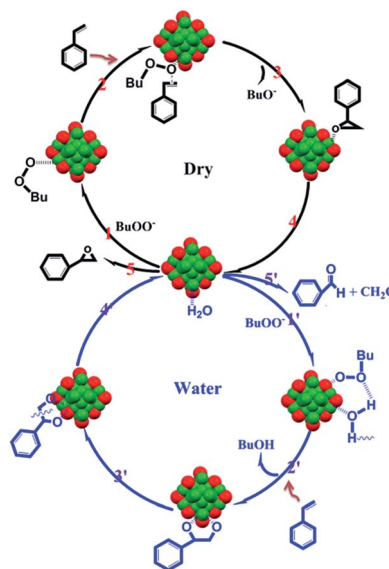


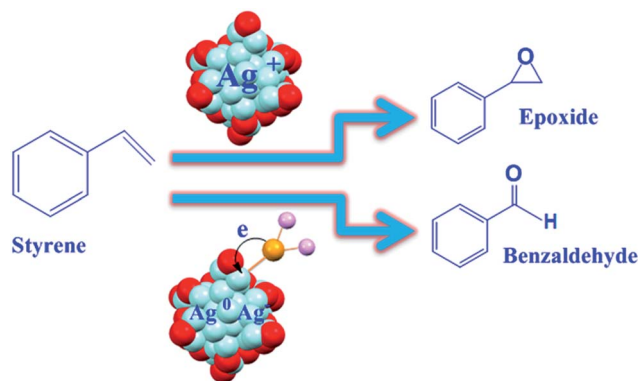
Fig. 6 XPS spectra of (a) Au 4f for $Au_{12}Ag_{32}/CNT$; (b) Ag 3d for $Au_{12}Ag_{32}/CNT$.



Scheme 2 Proposed mechanism for Au_{25} nanocluster catalyzed styrene oxidation of (black line for dry Au_{25}/CNT and blue line for soaked) (color labels: green = Au, red = S).

catalyst (Scheme 2 black line). Thereafter, the interaction with alkali (*i.e.* K_2CO_3 , which was added to facilitate TBHP activation) and styrene enables the formation of the ternary ring oxygen complex, from which the epoxide product can be released. However, when H_2O is present in the solvent, FT-IR spectrum of the Au_{25}/CNT catalyst displays a peak at $\sim 1630\text{ cm}^{-1}$ belonging to δOH of co-adsorbed water (as shown in Fig. 4b). Comparing the Au $4f_{7/2}$ XPS spectra of these two types of Au_{25}/CNT , we found that H_2O does not affect the valence state of Au, so we hypothesize that H_2O changes the surface of Au_{25} (Scheme 2 blue line). Both H_2O and oxidant TBHP bonded with catalyst Au_{25} , forming a pentacyclic oxygen complex. When styrene interacts with 2', its α -C easily connects with δOH (due to the steric hindrance of TBHP) and generates benzaldehyde as the primary product (Scheme 2 blue line). This mechanism is supported by the isotope labelling experiment, in which the ^{18}O benzaldehyde has been detected when the mixed solvent of $^{18}OH_2$ and toluene was used (with otherwise identical conditions as in Table 1 entry 5, see ESI† for the details of isotope experiments).

Compared to Au_{25} , the result of the styrene oxidation over the Ag_{44} catalyst is easier to understand. Combined with the



Scheme 3 Schematic illustration showing $\text{Ag}_{44}/\text{CNT}$ (with or without H_2O) nanocluster catalyzed styrene oxidation (color labels: light blue = Ag, red = S, golden = O and magenta = H).

experimental results and various characterization, the result of the styrene oxidation catalysed by $\text{Ag}_{44}/\text{CNT}$ is illustrated in Scheme 3. The water-free toluene was first chosen as the solvent. The binding energy for Ag $3d_{5/2}$ at 367.78 eV in $\text{Ag}_{44}/\text{CNT}$ is close to Ag^+ ,⁵⁴ and thus we suggest that $\text{Ag}_{44}/\text{CNT}$ acts as Ag^+ in the styrene oxidation to epoxide. By contrast, the presence of water shifts the Ag $3d$ peak of $\text{Ag}_{44}/\text{CNT}$ from 367.88 eV to 368.08 eV, and indicates the electron transfer from H_2O to Ag. According to the XPS analysis, we suggest that the Ag of reduced state (after soaking in water) catalyses the selective oxidation of styrene to benzaldehyde.

Compared with the homometal nanoclusters, the bimetallic $\text{Au}_{25-x}\text{Ag}_x/\text{CNT}$ catalysts could increase the selectivity and give much better conversion than the homosilver nanocluster. The FT-IR spectrum of the $\text{Au}_{25-x}\text{Ag}_x/\text{CNT}$ also exhibits a band centred at 1630 cm^{-1} after it is soaked by water (Fig. 4a), and XPS spectra show an increase of 0.6 eV than the dry sample. Although the valence state of Au in the $\text{Au}_{25-x}\text{Ag}_x/\text{CNT}$ is not affected by water, Au promotes the electron transfer from H_2O to Ag (binding energy shift, 0.3 eV vs. 0.6 eV). So the bimetallic $\text{Au}_{25-x}\text{Ag}_x/\text{CNT}$ -catalysed styrene oxidation showed better conversion and selectivity than the homogold and homosilver nanoclusters.

From the aforementioned results and discussions, we conclude that the changed selectivity from epoxide to benzaldehyde in styrene oxidation is caused by H_2O . In detail, water could change the surface composition of Au or the valence state of Ag. FT-IR analysis indicates that the water absorption occurs on the surface of all these catalysts. In particular, the product selectivity was not changed when water-treated $\text{Au}_{12}\text{Ag}_{32}/\text{CNT}$ was used as catalyst. Meanwhile, XPS shows no difference between the dry and soaked $\text{Au}_{12}\text{Ag}_{32}/\text{CNT}$. H_2O fails in changing the surface composition of Au because Au atoms are located as the kernel atoms in $\text{Au}_{12}\text{Ag}_{32}$. The kernel Au atoms also restrain the electron transfer from H_2O to Ag (binding energy shift, 0.3 eV in $\text{Au}_{25-x}\text{Ag}_x$ vs. 0 eV in $\text{Au}_{12}\text{Ag}_{32}$). Therefore, the special core-shell structure (Au_{12} kernel and Ag_{32} shell) of bimetallic $\text{Au}_{12}\text{Ag}_{32}$ nanocluster makes water useless.

4 Conclusion

This study presents the structure-determined catalytic results of homometal ($\text{Au}_{25}/\text{CNT}$ and $\text{Ag}_{44}/\text{CNT}$) and alloy nanoclusters ($\text{Au}_{25-x}\text{Ag}_x/\text{CNT}$ and $\text{Au}_{12}\text{Ag}_{32}/\text{CNT}$) for styrene selective oxidation by using TBHP as the oxygen source and toluene or mixed toluene/water as the solvent. The catalytic activity of bimetallic $\text{Au}_{25-x}\text{Ag}_x$ nanoclusters outperforms the homogold and homosilver (*i.e.*, higher conversion than homosilver and higher selectivity than homosilver). What is more important, it was found that the selectivity of styrene has been discovered to be controlled by an important factor – H_2O adsorbed on the surface of nanoclusters. The possible route for nanocluster-catalysed styrene selective oxidation with the action of water has been proposed. According to the experimental measurements, H_2O could change the surface composition of Au for Au_{25} nanocluster and the valence state of Ag for Ag_{44} nanoclusters. The advantages of both the silver and the gold have been well reflected on the surface of doped bimetallic $\text{Au}_{25-x}\text{Ag}_x$, while the core-shell structured bimetallic $\text{Au}_{12}\text{Ag}_{32}$ nanocluster gives no distinct result due to the inability of water in affecting either the composition of Au or the charge state of Ag. Overall, this study provides deep insight into the important of water in the selective styrene oxidation using nanocluster catalysts, which will be helpful for future mechanistic studies.

Conflict of interest

The authors declare no competing financial interests.

Acknowledgements

We acknowledge financial support from NSFC 21372006, 11374013 & U1532141, the Ministry of Education, the Education Department of Anhui Province, 211 Project of Anhui University.

Notes and references

- 1 R. Ferrando, J. Jellinek and R. L. Johnston, *Chem. Rev.*, 2008, **108**, 84.
- 2 C. Burda, X. Chen, R. Narayanan and M. A. El-Sayed, *Chem. Rev.*, 2005, **105**, 1025.
- 3 S. Yang, S. Wang, S. Jin, S. Chen, H. Sheng and M. Zhu, *Nanoscale*, 2015, **7**, 10005.
- 4 Y. Chen, Y. Zhou, H. Wang, J. Lu, T. Uchida, Q. Xu, S. Yu and H. Jiang, *ACS Catal.*, 2015, **5**, 2062.
- 5 F. Tao, M. E. Grass, Y. Zhang, D. R. Butcher, J. R. Renzas, Z. Liu, J. Y. Chung, B. S. Mun, M. Salmeron and G. A. Somorjai, *Science*, 2008, **322**, 932.
- 6 C. Chen, C. F. H. Byles, J. C. Buffet, N. H. Rees, Y. Wu and D. O'Hare, *Chem. Sci.*, 2016, **7**, 1457.
- 7 H. Lin, J. Zheng, X. Zheng, Z. Gu, Y. Yuan and Y. Yang, *J. Catal.*, 2015, **330**, 135.
- 8 Y. Shen, P. Hsu, B. Unnikrishnan, Y. Li and C. Huang, *ACS Appl. Mater. Interfaces*, 2014, **6**, 2576.
- 9 R. Liu, H. Huang, H. Li, Y. Liu, J. Zhong, Y. Li, S. Zhang and Z. Kang, *ACS Catal.*, 2014, **4**, 328.

- 10 B. Yang, R. Burch, C. Hardacre, G. Headdock and P. Hu, *ACS Catal.*, 2012, **2**, 1027.
- 11 H. Jiang, T. Akita, T. Ishida, M. Haruta and Q. Xu, *J. Am. Chem. Soc.*, 2011, **133**, 1304.
- 12 A. Steinbrück, A. Csáki, G. Festag and W. Fritzsche, *Plasmonics*, 2006, **1**, 79.
- 13 S. Wang, X. Meng, A. Das, T. Li, Y. Song, T. Cao, X. Zhu, M. Zhu and R. Jin, *Angew. Chem., Int. Ed.*, 2014, **53**, 2376.
- 14 N. Nishida, Y. Shiraishi, S. Kobayashi and N. Toshima, *J. Phys. Chem. C*, 2008, **112**, 20284.
- 15 H. Zhang, M. Jin and Y. Xia, *Chem. Soc. Rev.*, 2012, **41**, 8035.
- 16 H. Liu, F. Nosheen and X. Wang, *Chem. Soc. Rev.*, 2015, **44**, 3056.
- 17 H. Qian, D. Jiang, G. Li, C. Gayathri, A. Das, R. R. Gil and R. Jin, *J. Am. Chem. Soc.*, 2012, **134**, 16159.
- 18 S. Xie, H. Tsunoyama, W. Kurashige, Y. Negishi and T. Tsukuda, *ACS Catal.*, 2012, **2**, 1519.
- 19 F. Wang, W. Li, X. Feng, D. Liu and Y. Zhang, *Chem. Sci.*, 2016, **7**, 1867.
- 20 Y. Liu and S. Yang, *Electrochim. Acta*, 2007, **52**, 1925.
- 21 L. Chen, Y. Gao, H. Xu, Z. Wang, Z. Li and R. Zhang, *Phys. Chem. Chem. Phys.*, 2014, **16**, 20665.
- 22 R. Elghanian, J. J. Storhoff, R. C. Mucic, R. L. Letsinger and C. A. Mirkin, *Science*, 1997, **277**, 1079.
- 23 H. Qiu, L. Li, Q. Lang, F. Zou and X. Huang, *RSC Adv.*, 2012, **2**, 3548.
- 24 Y. Pei, G. Zhou, N. Luan, B. Zong, M. Qiao and F. Tao, *Chem. Soc. Rev.*, 2012, **41**, 8140.
- 25 S. V. Kershaw, A. S. Sussha and A. L. Rogach, *Chem. Soc. Rev.*, 2013, **42**, 3033.
- 26 C. Han, X. Yang, G. Gao, J. Wang, H. Lu, J. Liu, M. Tong and X. Liang, *Green Chem.*, 2014, **16**, 3603.
- 27 C. L. Bracey, P. R. Ellis and G. J. Hutchings, *Chem. Soc. Rev.*, 2009, **38**, 2231.
- 28 X. Guo, W. Ye, H. Sun, Q. Zhang and J. Yang, *Nanoscale*, 2013, **5**, 12582.
- 29 Y. C. Tsao, S. Rej, C. Y. Chiu and M. H. Huang, *J. Am. Chem. Soc.*, 2014, **136**, 396.
- 30 N. Sasirekha, P. Sangeetha and Y. W. Chen, *J. Phys. Chem. C*, 2014, **118**, 15226.
- 31 D. Tsukamoto, A. Shiro, Y. Shiraishi, Y. Sugano, S. Ichikawa, S. Tanaka and T. Hirai, *ACS Catal.*, 2012, **2**, 599.
- 32 C. Kumara, C. M. Aikens and A. Dass, *J. Phys. Chem. Lett.*, 2014, **5**, 461; Y. Negishi, T. Iwai and M. Ide, *Chem. Commun.*, 2010, **46**, 4713; D. R. Kauffman, D. Alfonso, C. Matranga, H. Qian and R. Jin, *J. Phys. Chem. C*, 2013, **117**, 7914; X. Dou, X. Yuan, Q. Yao, Z. Luo, K. Zheng and J. Xie, *Chem. Commun.*, 2014, **50**, 7459.
- 33 C. Kumara and A. Dass, *Nanoscale*, 2012, **4**, 4084; C. Kumara, K. J. Gagnon and A. Dass, *J. Phys. Chem. Lett.*, 2015, **6**, 1223.
- 34 J. Xiang, P. Li, Y. Song, X. Liu, H. Chong, S. Jin, Y. Pei, X. Yuan and M. Zhu, *Nanoscale*, 2015, **7**, 18278.
- 35 C. Kumara and A. Dass, *Nanoscale*, 2011, **3**, 3064.
- 36 H. Yang, Y. Wang, H. Huang, L. Gell, L. Lehtovaara, S. Malola, H. Häkkinen and N. Zheng, *Nat. Commun.*, 2013, **4**, 2422.
- 37 S. Wang, S. Jin, S. Yang, S. Chen, Y. Song, J. Zhang and M. Zhu, *Sci. Adv.*, 2015, **1**, e1500441.
- 38 C. Chang, Y. Wang and J. Li, *Nano Res.*, 2011, **4**, 131.
- 39 J. Zhu, J. L. Figueiredo and J. L. Faria, *Catal. Commun.*, 2008, **9**, 2395.
- 40 H. Tsunoyama, N. Ichikuni, H. Sakurai and T. Tsukuda, *J. Am. Chem. Soc.*, 2009, **131**, 7086.
- 41 S. Lee, L. M. Molina, M. J. Lpez, J. A. Alonso, B. Hammer, B. Lee, S. Seifert, R. E. Winans, J. W. Elam, M. J. Pellin and S. Vajda, *Angew. Chem., Int. Ed.*, 2009, **48**, 1467.
- 42 A. Villa, N. Janjic, P. Spontoni, D. Wang, D. Su and L. Prati, *Appl. Catal., A*, 2009, **364**, 221.
- 43 Y. Guan and E. J. M. Hensen, *Appl. Catal., A*, 2009, **361**, 49.
- 44 C. Shang and Z. Liu, *J. Am. Chem. Soc.*, 2011, **133**, 9938.
- 45 C. Chang, X. Yang, B. Long and J. Li, *ACS Catal.*, 2013, **3**, 1693.
- 46 X. Nie, C. Zeng, X. Ma, H. Qian, Q. Ge, H. Xua and R. Jin, *Nanoscale*, 2013, **5**, 5912.
- 47 X. Nie, H. Qian, Q. Ge, H. Xu and R. Jin, *ACS Nano*, 2012, **6**, 6014.
- 48 M. Zhu, E. Lanni, N. Garg, M. E. Bier and R. Jin, *J. Am. Chem. Soc.*, 2008, **130**, 1138; M. Zhu, C. M. Aikens, F. J. Hollander, G. C. Schatz and R. Jin, *J. Am. Chem. Soc.*, 2008, **130**, 5883.
- 49 D. Crasto, S. Malola, G. Brosofsky, A. Dass and H. Häkkinen, *J. Am. Chem. Soc.*, 2014, **136**, 5000.
- 50 P. Huang, G. Chen, Z. Jiang, R. Jin, Y. Zhu and Y. Sun, *Nanoscale*, 2013, **5**, 3668.
- 51 Y. Zhu, H. Qian, M. Zhu and R. Jin, *Adv. Mater.*, 2010, **22**, 1915.
- 52 Y. Zhu, H. Qian and R. Jin, *Chem.-Eur. J.*, 2010, **16**, 11455.
- 53 G. S. Foo, D. Wei, D. S. Sholl and C. Sievers, *ACS Catal.*, 2014, **4**, 3180.
- 54 Y. Negishi, T. Iwai and M. Ide, *Chem. Commun.*, 2010, **46**, 4713.